

2016

# Estimation of Uncertainty in Air-Water Exchange Flux and Gross Volatilization Loss of PCBs: a Case Study based on Passive Sampling in the Lower Great Lakes

Ying Liu

Siyao Wang

*See next page for additional authors*

Follow this and additional works at: <https://digitalcommons.uri.edu/gsofacpubs>

**The University of Rhode Island Faculty have made this article openly available.  
Please let us know how Open Access to this research benefits you.**

This is a pre-publication author manuscript of the final, published article.

Terms of Use

This article is made available under the terms and conditions applicable towards Open Access Policy Articles, as set forth in our [Terms of Use](#).

## Citation/Publisher Attribution

Liu, Y., Wang, S., McDonough, C. A., Khairy, M., Muir, D., & Lohmann, Rainer. (2016). Estimation of Uncertainty in Air-Water Exchange Flux and Gross Volatilization Loss of PCBs: A Case Study Based on Passive Sampling in the Lower Great Lakes. *Environmental Science & Technology*, 50(20), 10894-10902.

Available at: <http://pubs.acs.org/doi/abs/10.1021/acs.est.6b02891>

This Article is brought to you for free and open access by the Graduate School of Oceanography at DigitalCommons@URI. It has been accepted for inclusion in Graduate School of Oceanography Faculty Publications by an authorized administrator of DigitalCommons@URI. For more information, please contact [digitalcommons@etal.uri.edu](mailto:digitalcommons@etal.uri.edu).

---

**Authors**

Ying Liu, Siyao Wang, Carrie A. McDonough, Mohammed Khairy, Derek Muir, and Rainer Lohmann

1 **Estimation of Uncertainty in Air-Water Exchange Flux**  
2 **and Gross Volatilization Loss of PCBs: a Case Study**  
3 **based on Passive Sampling in the Lower Great Lakes.**

4

5 YING LIU<sup>†,‡,\*</sup>, SIYAO WANG<sup>†</sup>, CARRIE A. MCDONOUGH<sup>‡</sup>, MOHAMMED KHAIRY<sup>‡,ϕ</sup>,  
6 DEREK MUIR<sup>§</sup>, RAINER LOHMANN<sup>‡,\*</sup>

7

8 <sup>†</sup> *State Key Laboratory of Pollution Control and Resource Reuse, Shanghai Key Lab*  
9 *of Chemical Assessment and Sustainability, College of Environmental Science*  
10 *and Engineering, Tongji University, Shanghai 200092, China.*

11 <sup>‡</sup> *Graduate School of Oceanography, University of Rhode Island, Narragansett,*  
12 *Rhode Island 02882-1197, United States.*

13 <sup>ϕ</sup> *Department of Environmental Sciences, Faculty of Science, Alexandria University,*  
14 *21511 Moharam Bek, Alexandria, Egypt.*

15 <sup>§</sup> *Environment Canada, Atmosphere, Water, and Soil Contaminant Dynamics, 867*  
16 *Lakeshore Road, Burlington, Ontario L7R 4A6, Canada.*

17

18 \* To whom correspondence should be addressed

19 E-mail address: rlohmann@mail.uri.edu (R. Lohmann), Phone: 401-874-6612,

20 Fax: 401-874-6811; liu\_ying@tongji.edu.cn (Y. Liu).

21 **ABSTRACT**

22 Compared with dry and wet deposition fluxes, air-water exchange flux cannot  
23 be directly measured experimentally. Its model-based calculation contains  
24 considerable uncertainty because of uncertainties in input parameters. To  
25 capture inherent variability of air-water exchange flux of PCBs across the lower  
26 Great Lakes and calculate their annual gross volatilization loss, 57 pairs of air  
27 and water samples from 19 sites across Lakes Erie and Ontario were collected  
28 using passive sampling technology during 2011-2012. Error propagation  
29 analysis and Monte Carlo simulation were applied to estimate uncertainty in the  
30 air-water exchange fluxes. Results from both methods were similar, but error  
31 propagation analysis estimated smaller uncertainty than Monte Carlo simulation  
32 in cases of net deposition. Maximum likelihood estimations (MLE) on wind speed  
33 and air temperature were recommended to quantify the site-specific air-water  
34 exchange flux. An assumed 30-40% of relative uncertainty in overall air-water  
35 mass transfer velocity was confirmed. MLEs on volatilization fluxes of total PCBs  
36 across Lakes Erie and Ontario were  $0.78 \text{ ng m}^{-2} \text{ day}^{-1}$  and  $0.53 \text{ ng m}^{-2} \text{ day}^{-1}$ ,  
37 respectively, and gross volatilization losses of total PCBs over the whole lakes  
38 were  $74 \text{ kg year}^{-1}$  for Lake Erie and  $63 \text{ kg year}^{-1}$  for Lake Ontario. Mass balance  
39 analysis across Lake Ontario indicated that volatilization was an uppermost loss  
40 process of aqueous PCBs.

41 **INTRODUCTION**

42 Polychlorinated biphenyls (PCBs) are a class of persistent toxic chemical  
43 substances of concern in the Great Lakes.<sup>1-3</sup> Atmospheric deposition was  
44 considered as a significant source of PCBs to the lower Great Lakes, including dry  
45 deposition, wet deposition and air-water diffusive fluxes.<sup>4, 5</sup> Atmospheric  
46 processes accounted for 80-90% of total loadings of PCBs to the oceans and 65%  
47 of total atmospheric deposition of PCBs was attributed to gas transfer.<sup>6</sup> Results  
48 from Lake Superior revealed that volatilization was a major loss process of PCBs  
49 from water column and gross volatilization loss of PCBs was 250 kg year<sup>-1</sup> for  
50 1992.<sup>7</sup> Across Lakes Erie and Ontario, net volatilization from lake waters was  
51 still a primary trend of PCB gas exchange process in our previous work.<sup>8</sup> In  
52 previous publications, air-water exchange fluxes of PCBs had been estimated, but  
53 with limited knowledge on its uncertainty,<sup>6, 7, 9-11</sup> especially involving variations  
54 of the flux over time and space.

55 Compared with dry and wet deposition fluxes, air-water (diffusive) exchange  
56 flux cannot be directly measured experimentally and its calculation (based on a  
57 two-film diffusion model) involves air vapor and freely-dissolved water  
58 concentrations, air-water partitioning and air-water mass transfer coefficients of  
59 PCBs.<sup>10, 12, 13</sup> The gaseous and freely-dissolved PCBs are not bound to particulates  
60 by definition, and the filtered air or water in active sampling is only operationally  
61 defined as gaseous or dissolved, as any particles penetrating the filters are also  
62 included.<sup>14, 15</sup> By contrast, passive sampling is an ideal technology for air-water  
63 exchange flux measurements, because it specifically captures the gaseous and  
64 freely-dissolved fractions, avoiding the filter bias.<sup>11</sup> Nonetheless, passive  
65 sampling contains uncertainties from PCB analysis and model coefficients, which

66 propagate in the air-water exchange flux calculations.

67 Error propagation analysis is a common method to estimate flux uncertainty,  
68 and many researchers have applied this method to quantify the uncertainty, e.g.,  
69 in the Lakes Erie and Ontario,<sup>8, 16</sup> in the Lake Superior,<sup>16, 17</sup> in the Chesapeake  
70 Bay,<sup>14</sup> in Taiwanese coasts,<sup>18, 19</sup> and in East China Sea.<sup>20</sup> These studies assumed  
71 relative uncertainties of approximately 50% for Henry's law constants, around  
72 30-40% for air-water mass transfer velocities of PCBs and a normal distribution  
73 of the flux. But the flux does not always follow a normal distribution (see below)  
74 because not all of uncertainties in model parameters (e.g., wind speed and  
75 air-water transfer velocity of PCBs) contain a random error. An alternative  
76 method is the use of Monte Carlo simulations. The technique can quantify the  
77 effect of uncertainty from varying parameters on model result.<sup>21</sup> Venier and  
78 Hites estimated total net mass transfer rates of PBDEs to the Great Lakes and  
79 their relative errors using the simulations; however, the calculated results were  
80 based on only one to five samples per lake and variables were assumed to follow  
81 a normal distribution.<sup>22</sup> Qin et al. fitted probability distribution of variables by  
82 normal or lognormal distribution functions, but ignored their potential  
83 correlations (e.g., between gaseous and aqueous concentrations).<sup>15</sup> To our  
84 knowledge, few studies have evaluated the uncertainty and parameter sensitivity  
85 in air-water exchange flux of PCBs via Monte Carlo simulation. Furthermore,  
86 many studies estimated uncertainty in the flux based on only a few sampling  
87 sites due to limited deployments,<sup>7, 17, 18</sup> yet atmospheric and aqueous  
88 concentrations of PCBs and meteorology situation are significantly varying over  
89 time and space,<sup>8</sup> resulting in temporal and spatial variations of air-water  
90 exchange flux across the whole lakes and enormous uncertainty in annual gas

91 transfer loadings of PCBs. This prompted us to comprehensively estimate overall  
92 uncertainty in air-water exchange flux of PCBs across the lakes.

93 To capture the inherent variation in air-water exchange of PCBs, a case study  
94 across Lakes Erie (31 pair air and water samples from 9 sampling sites) and  
95 Ontario (26 pairs from 10 sites) was performed based on passive sampling  
96 during 2011-2012.<sup>8,23</sup> Error propagation analysis and Monte Carlo simulation  
97 were conducted to estimate uncertainty in air-water exchange flux of PCBs. The  
98 aim of this study includes 1) estimating uncertainty in air-water exchange  
99 equilibrium of PCBs, 2) comparing results from both methods, and 3) evaluating  
100 uncertainty in air-water exchange fluxes and annual gross volatilization loss of  
101 PCBs across both lakes.

102

## 103 **MATERIALS AND METHODOLOGY**

104 **Passive sampling and chemical analysis.** The information on sampling sites,  
105 low density polyethylene (LDPE) deployment in air and water, chemical analysis  
106 methodologies and preparation of the LDPE passive samplers, quality assurance  
107 and quality control were described elsewhere.<sup>8</sup> Briefly, the LDPE membranes  
108 were spiked with performance reference compounds, and deployed in the air  
109 and water of Lakes Erie and Ontario. In this study, uncertainty in air-water  
110 exchange flux of PCBs was estimated based on 57 pair samples (air and water)  
111 collected during 2011-2012, nine sites from Lake Erie and ten sites from Lake  
112 Ontario, as shown in Figure S1. After collection, LDPE samples were spiked with  
113 surrogate standards (<sup>13</sup>C labeled PCBs), extracted and cleaned up if needed. 29  
114 PCB congeners (CB 8, 11, 18, 28, 44, 52, 66, 77, 81, 101, 105, 114, 118, 123, 126,  
115 128, 138, 153, 156, 157, 167, 169, 170, 180, 187, 189, 195, 206, 209) were

116 analyzed using GC-MS/MS. Procedural blanks, field blanks, matrix spikes, and  
 117 duplicate samples were involved in the analysis. Limits of detection, recoveries  
 118 and relative standard deviations of target PCBs were reported elsewhere.<sup>8</sup> The  
 119 related meteorological data are presented in Table S1.

120 **Air-water fugacity ratio.** The fugacity ratio ( $f_a/f_w$ ) is normally calculated  
 121 from atmospheric and aqueous concentrations of PCBs ( $C_a$  and  $C_w$ , both in  $\text{pg m}^{-3}$ )  
 122 and (air) temperature-corrected partitioning coefficient between air and water  
 123 ( $K_{aw}$ ), as shown in Equation 1.

$$124 \quad \log\left(\frac{f_a}{f_w}\right) = \log\left(\frac{C_a}{C_w \times K_{aw}}\right) \quad (1)$$

125 Based on the LDPE passive sampling technology,<sup>24</sup> the atmospheric and  
 126 aqueous concentrations ( $C_a$  and  $C_w$ ) can be calculated according to equilibrium  
 127 concentrations of PCBs measured in the deployed LDPE sheets (based on LDPE  
 128 volume) and partitioning coefficients between LDPE and air or water ( $K_{PE-a(w)}$ ),  
 129 as presented in Equation 2. Hence, the fugacity ratio depends only on the  
 130 equilibrium concentrations of PCBs in LDPE matrix (deployed in air and water),  
 131 as shown in Equation 3.

$$132 \quad C_{a(w)} = \frac{C_{PE}}{\%equ(a/w) \times K_{PE-a(w)}} \quad (2)$$

$$133 \quad \log\left(\frac{f_a}{f_w}\right) = \log\left(\frac{C_a}{C_w \times K_{aw}}\right) = \log\left(\frac{C_{PE(a)}}{\%equ(a) \times K_{PE-a}} \times \frac{\%equ(w) \times K_{PE-w}}{C_{PE(w)} \times K_{aw}}\right) = \log\left(\frac{C_{PE(a)}}{C_{PE(w)}} \times \frac{\%equ(w)}{\%equ(a)}\right) \quad (3)$$

134 where %equ is the predicted percent equilibrium (for more detail see the SI).

135 **Air-water exchange flux.** The flux ( $F_{a/w}$ , in  $\text{pg m}^{-2} \text{ day}^{-1}$ ) is commonly  
 136 calculated from overall air-water mass transfer velocity ( $v_{a/w}$ , in  $\text{m day}^{-1}$ ) and the  
 137 concentration difference between water and air ( $C_w - C_a/K_{aw}$ ) as in Equation 4,<sup>10, 17</sup>  
 138 where  $K_{aw}$  is air-water partitioning coefficient corrected by (air) temperature.

$$139 \quad F_{a/w} = v_{a/w} \times (C_w - C_a/K_{aw}) \quad (4)$$



140  $K_{aw}$  is determined as Equation 5, where  $H_c$  is Henry's law constant (in atm L  
141 mol<sup>-1</sup>),  $R$  is the gas constant (0.08206 in atm L mol<sup>-1</sup> K<sup>-1</sup>), and  $T$  is the absolute  
142 temperature in Kelvin.  $H_c$  values were obtained from Khairy et al.<sup>25</sup>

$$143 \quad K_{aw} = \frac{H_c}{R \times T} \quad (5)$$

144 Overall mass transfer velocity ( $v_{a/w}$ ) was calculated based on a modified  
145 two-film air-water exchange model,<sup>10</sup> equated as follows,

$$146 \quad \frac{1}{v_{a/w}} = \frac{1}{v_w} + \frac{1}{K_{aw} \times v_a} \quad (6)$$

147 where  $v_a$  and  $v_w$  are the air-side and water-side transfer velocities of target  
148 compound, respectively. They are a function of the molecular diffusivity of the  
149 target compound in air or water and stability-dependent turbulent diffusivity  
150 (wind speed).<sup>10</sup>

151 **Error propagation analysis.** In order to estimate the uncertainty in air-water  
152 fugacity ratio and the calculated diffusive flux using statistical techniques,  
153 measured uncertainties in air and water analysis, air-water partitioning  
154 coefficients (including Henry's law constant and temperature) and overall mass  
155 transfer velocity were considered.

156 There are four variables with random uncertainty for the fugacity ratio based  
157 on Equations 1 and 5, for which the error propagation is given in Equation 7.  
158 With regard to the passive sampling technology, four variables are involved (see  
159 Equation 3); its error propagation is detailed in Equation 8. Relative uncertainty  
160 of percent equilibrium was estimated in the Supporting Information and ranges  
161 from 0% to 51% (Table S2),

$$162 \quad \delta \log \left( \frac{f_a}{f_w} \right) = \sqrt{\left( \frac{\delta C_a}{C_a} \right)^2 + \left( \frac{\delta C_w}{C_w} \right)^2 + \left( \frac{\delta H_c}{H_c} \right)^2 + \left( \frac{\delta T}{T} \right)^2} \quad (7)$$

$$\delta \log \left( \frac{f_a}{f_w} \right) = \sqrt{\left( \frac{\delta C_{PE(a)}}{C_{PE(a)}} \right)^2 + \left( \frac{\delta C_{PE(w)}}{C_{PE(w)}} \right)^2 + \left( \frac{\delta \%equilibrium(a)}{\%equilibrium(a)} \right)^2 + \left( \frac{\delta \%equilibrium(w)}{\%equilibrium(w)} \right)^2} \quad (8)$$

Error propagation analysis was applied to the air-water exchange flux given by Equation 4 and 5, yielding the following:

$$\frac{\delta F}{F} = \sqrt{\left( \frac{\delta v_{a/w}}{v_{a/w}} \right)^2 + \left( \frac{v_{a/w} C_a R T}{F H_c} \frac{\delta H_c}{H_c} \right)^2 + \left( \frac{v_{a/w} C_a R}{F H_c} \delta T \right)^2 + \left( \frac{v_{a/w} R T}{F H_c} \delta C_a \right)^2 + \left( \frac{v_{a/w}}{F} \delta C_w \right)^2} \quad (9)$$

The relative standard deviations (RSD) of atmospheric and aqueous concentrations ( $\frac{\delta C_a}{C_a}$  and  $\frac{\delta C_w}{C_w}$ ) are associated with the analysis and obtained from Table S2. A value of 30% and 50% was assumed for RSDs in  $v_{a/w}$  and  $H_c$ , respectively, after Rowe and Perlinger.<sup>17</sup> The standard deviation ( $\delta$ ) in T was calculated based on the NOAA National Data Buoy Center historical archives ([www.ndbc.noaa.gov](http://www.ndbc.noaa.gov)). A detailed description of error propagation analysis is presented in the Supporting Information.

**Monte Carlo simulation.** This was performed for the overall air-water mass transfer velocity ( $v_{a/w}$ ) and air-water exchange flux ( $F_{a/w}$ ) of PCBs for each sample pair. The general method is to quantify uncertainty associated with incomplete data (e.g., wind speed, ambient temperature, atmospheric and aqueous PCB concentrations) by model-fitting probability distribution functions (PDF) of the incomplete data that are used as input to Monte Carlo simulations. We fitted fourteen available PDFs to derive the best-fit PDF of site-specific ambient parameters. The best-fit PDFs and probability charts were used to generate a set of random values for input parameters. As variables in the system being modeled are often inter-dependent, we defined correlations between ambient temperature and wind speed based on pairs of measured data. Normal

185 distributions with specified ranges were assumed for other parameters,  
186 including atmospheric and aqueous PCB concentrations and Henry's law  
187 constants of PCBs. Standard deviation of the PCB concentrations were set to the  
188 product of average relative standard deviation and site-specific PCB  
189 concentrations. Relative uncertainty in  $H_c$  was assumed as 50% after Blanchard  
190 et al. and Rowe et al.<sup>17, 26</sup> Finally, Monte Carlo simulations were applied for the  
191 estimation of air-water exchange of PCBs across the whole lakes over time and  
192 place. Passive sampling data from 2011-2012 was used to construct PDFs of  
193 gaseous and freely-dissolved PCB concentrations across Lakes Erie and Ontario.  
194 Meteorological data from open lake sites were selected as representative air  
195 temperatures and wind speeds. Correlations between variables were carefully  
196 defined based on the monitoring data, including between atmospheric and  
197 aqueous concentrations and between PCB congeners. In each simulation, a total  
198 of  $10^5$  trials were generated to obtain sufficient data to estimate probability  
199 distributions of  $v_{a/w}$  and  $F_{a/w}$ . All simulations were performed using Oracle  
200 Crystal Ball R11.1 software packages. More details are presented in the  
201 Supporting Information.

202 **Gross volatilization loss and mass balance of PCBs.** Gross volatilization  
203 losses of PCBs across Lakes Erie and Ontario were calculated as the product of  
204 lake area and arithmetic mean of air-water exchange flux. Input (river inflows  
205 and precipitation) and output (river outflow and volatilization loss) of  
206 freely-dissolved PCBs into and from Lake Ontario were calculated for  
207 construction of whole lake mass balance. (see the Supporting Information for  
208 details).

209

## 210 **RESULTS AND DISCUSSION**

211 **Estimation of air-water exchange equilibrium of PCBs.** Most semi-volatile  
212 organic pollutants (e.g. PCBs) have the potential to migrate between air and  
213 water phases. The fugacity gradient of chemicals is a mathematical expression  
214 that describes the direction in which chemicals diffuse, or are transported  
215 between environmental compartments.<sup>27-29</sup> Fugacity is identical to partial  
216 pressure in ideal gases and is logarithmically related to chemical potential.  
217 Air-water fugacity ratios have been widely employed to determine net  
218 deposition ( $f_a/f_w > 1$ ), net volatilization ( $f_a/f_w < 1$ ), and equilibrium situation  
219 ( $f_a/f_w = 1$ ) in many works.<sup>9, 25, 30-33</sup> However, it is crucial to distinguish  
220 equilibrium from non-equilibrium situations in such multi-compartment  
221 exchange.<sup>34</sup> The range of fugacity ratios not significantly different from  
222 equilibrium can be estimated based on their uncertainty.<sup>9, 35, 36</sup> Uncertainty  
223 ranges of water-air exchange were calculated from Equations 7 and 8,  
224 respectively. Air-water fugacity ratios and the equilibrium ranges of selected  
225 PCBs are illustrated in Figure 1. Fugacity ratios were widely distributed, ranging  
226 from deposition to volatilization. It is challenging to accurately divide them into  
227 equilibrium and non-equilibrium situations. As for lighter PCBs (for example CB  
228 28 and 52), the equilibrium ranges based on Equation 8 were more narrow than  
229 those based on Equation 7. For active sampling (i.e., a direct measurement of  
230 atmospheric and aqueous concentrations which is considered here as a  
231 theoretical comparison), relative uncertainty (RU) in atmospheric and aqueous  
232 concentrations, ambient temperature and Henry's law constant were considered,  
233 as shown in Equation 7. In this study,  $0.29 < f_a/f_w < 3.47$  (or  $\text{RU in log}(f_a/f_w) =$   
234  $0.54$ ) were considered to not significantly differ from phase equilibrium. The

235 result is similar with previous reports, in which an equilibrium window  $0.3 <$   
236  $f_a/f_w < 3.0$  were accepted by Lammel et al.,<sup>35</sup> Lin et al.,<sup>20</sup> Mulder et al.,<sup>32</sup> Zhong et  
237 al.,<sup>31, 37</sup> Castro-Jimenez et al.,<sup>30</sup> and Lohmann et al.<sup>36</sup> In the passive sampling  
238 technique (see Equation 8), percent equilibrium reached (%equilibrium)  
239 replaces  $H_c$  and temperature. The %equilibrium depends on deployment time  
240 and turbulence in the environmental matrix. For lighter PCBs, the RUs  
241 in %equilibrium were lower, as congeners equilibrated in the field ( $\sim 100\%$   
242 of %equilibrium), whereas for heavier PCBs, the RUs in %equilibrium reached  
243 up to 51%, as those congeners attained  $< 20\%$  of %equilibrium (see Table S2).  
244 For dichlorobiphenyl, the RU in  $\log(f_a/f_w)$  reduced from 0.54 (Equation 7) to  
245 0.26 (namely  $0.55 < f_a/f_w < 1.82$ , for Equation 8). It reveals the advantage of the  
246 passive sampling technique in estimating non-equilibrium situation of air-water  
247 exchange of lighter PCBs. With regard to the congeners heavier than  
248 tetrachlorobiphenyl, however, the advantage gradually disappears because of  
249 greater RU in %equilibrium, as shown in Table S2. Generally speaking, across the  
250 lower Great Lakes, net volatilization of PCBs from water to air was a primary  
251 trend in most cases (accounting for 53-78% of total samples), except for CB 118  
252 and 180.

253 Meanwhile, the probability of deposition or volatilization was also computed  
254 via Monte Carlo simulation in this study (as discussed in the following section).  
255 Table 1 lists air-water fugacity ratios and confidence levels of net deposition or  
256 volatilization of 7 selected PCBs for a specific sample (deployed at the Cape  
257 Vincent site in 2012 autumn). If a probability value was greater than 90% (hence  
258 tail probability was less than 10%), we were quite confident of air-water  
259 exchange direction. As shown in Table 1, the estimation of air-water exchange

260 direction based on Monte Carlo simulation are comparable or identical with  
261 those from the uncertainties in air-water fugacity ratios. Consequently, the  
262 Monte Carlo simulation further supports that the air-water fugacity ratios with  
263 uncertainty analysis based on the LDPE passive sampling technology is a simple  
264 and credible tool in estimating direction of air-water exchange of PCBs.

265 **Effect of parameterization on air-water exchange flux.** The flux ( $F_{a/w}$ ) is  
266 related to many parameters, including overall air-water mass transfer velocity  
267 ( $v_{a/w}$ ) and concentration difference in the water and air ( $C_w - C_a / K_{aw}$ ). Overall the  
268 transfer velocity depends on wind speed and temperature in the Whitman  
269 two-film model.<sup>10, 12</sup> The air-water partitioning coefficient ( $K_{aw}$ ) of compounds of  
270 interest was calculated based on the Henry's law constant ( $H_c$ ) and ambient  
271 temperature ( $T$ ). Hence, it is necessary to explore the effect of parameterization  
272 on air-water exchange flux.

273 We compared the difference of two parametric methods on ambient  
274 temperature and wind speed, i.e., arithmetic mean and maximum likelihood  
275 estimation (MLE) from best-fit probability distribution function (PDF).  
276 Probability distributions of ambient temperature, wind speed, overall mass  
277 transfer velocity, and air-water exchange flux from the Monte Carlo simulation  
278 are illustrated in Figure 2. Ambient temperatures followed a Weibull distribution  
279 (see Figure 2.b), and average temperature (13.56°C) was close to its MLE  
280 (14.36°C) from best-fit PDF. Wind speeds followed a lognormal distribution (see  
281 Figure 2.c), and average wind speed (5.14 m s<sup>-1</sup>) was much greater than its MLE  
282 (2.89 m s<sup>-1</sup>). The  $v_{a/w}$  is a piecewise function of wind speed after Schwarzenbach  
283 et al.<sup>10</sup> In this case, arithmetic mean and MLE of wind speed were in different  
284 sub-domains, leading to a great difference in the  $v_{a/w}$  values, as marked in Figure

285 2.d. The probability distribution pattern of  $F_{a/w}$  was similar to that of  $v_{a/w}$ . Both of  
286 them have a sharp peak with a large tail. MLEs of the  $F_{a/w}$  ( $0.62 \text{ ng m}^{-2} \text{ day}^{-1}$ ) and  
287 the  $v_{a/w}$  ( $19 \text{ cm day}^{-1}$ ) are close to the model calculated values based on MLEs of  
288 temperature and wind speed (see Figure 2.a and d). However, the  $F_{a/w}$  value  
289 ( $1.77 \text{ ng m}^{-2} \text{ day}^{-1}$ ) and the  $v_{a/w}$  value ( $53 \text{ cm day}^{-1}$ ) calculated from arithmetic  
290 mean (in the large tail) were  $\sim 2.5$  times greater than the MLE values. Hence, the  
291 MLEs of meteorological parameters are recommended according to the  
292 probability distributions of  $v_{a/w}$  and  $F_{a/w}$ . Due to the assumption that PCB  
293 concentrations in air and water followed a normal distribution with limited  
294 relative uncertainties (11-53%), uncertainty in  $F_{a/w}$  in the non-equilibrium  
295 situation depended mainly on the uncertainty in  $v_{a/w}$ . Consequently, the  
296 parametrization of ambient temperature and wind speed needs to be carefully  
297 evaluated when computing the air-water exchange flux of PCBs.

298 For most samples in this study, probability distribution patterns of  
299 meteorological data are similar to the above case (see Table S1). Briefly,  
300 temperature data followed a Weibull, Beta, or normal distribution, and in most  
301 cases MLE was close to its arithmetic mean. In contrast, wind speed data  
302 followed a lognormal distribution; the arithmetic mean likely overestimated  
303 wind speed and hence the air-water exchange flux. This applies both to daily  
304 sampling (as in active) as well as monthly samples (as in passive sampling).

305 **Estimation of uncertainty in air-water exchange flux.** The air-water  
306 exchange flux was quantified based on the two-film transfer model and relevant  
307 monitoring data. Uncertainties are inherent in measured data due to  
308 measurement limitations of PCB concentrations in air and water (e.g., sampling  
309 uncertainty and instrument precision) and temporal variations of wind speed

310 and ambient temperature, which propagate to the calculated flux. Since  
311 uncertainty calculations are based on statistics, there are different ways to  
312 determine overall uncertainty. In this study, we applied two methods to estimate  
313 the uncertainty in air-water exchange flux, i.e., error propagation analysis and  
314 Monte Carlo simulation.

315 *Uncertainty in overall air-water mass transfer velocity.* The transfer velocity of  
316 PCBs in air-water exchange was calculated with piecewise functions of wind  
317 speed in the two-film model. Error propagation analysis failed to capture the  
318 effect of uncertainty in wind speed on the uncertainty in the transfer velocity. In  
319 other studies, RSD of the transfer velocity were selected as 30% or 40%.<sup>17, 19, 26, 38</sup>  
320 In this study, we estimated the uncertainty in ( $v_{a/w}$ ) via Monte Carlo simulation.  
321 In Figure 2.d, a peak range (baseline width of peak) of  $v_{a/w}$  value is defined as a  
322 confidence interval with a specific certainty or a range of values that act as good  
323 estimate on the  $v_{a/w}$ . In this case, the 47.7% confidence interval of the  $v_{a/w}$  is  
324 12-25 cm day<sup>-1</sup> with MLE of 19 cm day<sup>-1</sup>.

325 In the fourteen selected samples across Lakes Erie and Ontario (see Figure S2),  
326 uncertainty results of  $v_{a/w}$  from Monte Carlo simulation are similar to an  
327 assumed 30% of relative uncertainty (RU). In most cases, MLEs of  $v_{a/w}$  from  
328 Monte Carlo simulation (red open squares) are close to mode values based on  
329 MLEs of wind speed and temperature (blue open circles). Moreover, peak ranges  
330 from Monte Carlo simulation are similar to those with 30% of RU in  $v_{a/w}$ .  
331 Certainties in these peak ranges are 46%-78% in these samples. Therefore, it is  
332 reasonable to select 30-40% as the RU in  $v_{a/w}$ .

333 *Uncertainty in air-water exchange flux.* The uncertainty was estimated  
334 quantitatively by Monte Carlo simulation, and Figure 2.a presents probability



335 distribution of air-water exchange flux of  $\Sigma_7$ PCBs as an example. The probability  
336 distribution follows a sharp peak with a large tail towards larger values (right  
337 side). The large tailing mostly resulted from the lognormal probability  
338 distribution of wind speed data. The flux range between 10% and 90%  
339 percentiles covered a wide range of 0.36-5.1 ng m<sup>-2</sup> day<sup>-1</sup>. However, the baseline  
340 width of the probability peak (i.e., 0.26-0.95 ng m<sup>-2</sup> day<sup>-1</sup>) is mainly located  
341 between the percentiles of 10%-50%. Even the middle 40% estimation of the  
342 flux (i.e., 0.56-2.1 ng m<sup>-2</sup> day<sup>-1</sup> for 30-70% estimation) overestimated the peak  
343 range of the flux. Therefore, the peak range can be defined as a good estimation  
344 range of the flux in this case, namely 0.26-0.95 ng m<sup>-2</sup> day<sup>-1</sup> with a 46.8%  
345 confidence level.

346 Meanwhile, error propagation analysis was also applied to determine  
347 uncertainty in the flux, based on the above conclusion that the 30% of RU in  $v_{a/w}$   
348 is reasonable approximation. The results from both methods for the fourteen  
349 selected samples are compared pair-wise and summarized in Figure 3. Best  
350 estimate values (open) of the flux were comparable and close to each other. Yet  
351 the good estimation ranges of air-water exchange fluxes were slightly different.  
352 In particular, when the air-water exchange displayed net volatilization or  
353 approached equilibrium, the uncertainty ranges from both methods were  
354 comparable each other. However, when the trend presented net deposition (e.g.,  
355 cases E03-3924 and On12-3503), the good estimation ranges from Monte Carlo  
356 simulation were obviously much wider than those from error propagation  
357 analysis. In particular, the lower boundaries of the exchange fluxes (or upper  
358 boundary of net deposition fluxes) from Monte Carlo simulation were much  
359 lower than those from error propagation analysis. A potential reason is that

360 uncertainties in input data have different contributions to the uncertainty in the  
361 flux in different exchange trends (see below).

362 Generally speaking, both methods determine the uncertainty range of  
363 air-water exchange flux of PCBs in the situations of net volatilization and  
364 approaching phase equilibrium well. However, Monte Carlo simulation is more  
365 precise, but more complex, than error propagation analysis. Error propagation  
366 analysis is a simple method to determine uncertainty in net volatilization flux,  
367 but is not recommended in net deposition situation, in which case Monte Carlo  
368 simulations should ideally be used.

369 *Parameters sensitivity analysis.* Probability distributions of air-water exchange  
370 flux were close to symmetrical distributions when air-water exchange  
371 approached equilibrium (see Figures S3.c and S3.d), while those in  
372 non-equilibrium situations showed positive skew (volatilization) or negative  
373 skew (deposition) distribution, as shown in Figure S3. Parameter sensitivity  
374 analysis can be employed to decide which parameters should be optimized or  
375 determined more accurately through further modeling or experimental studies.  
376 Hence, parameter sensitivity analysis was performed to study how the  
377 uncertainty in air-water exchange flux related to different sources of  
378 uncertainties in its input data, including atmospheric and aqueous  
379 concentrations, the Henry's law constant, ambient temperature and wind speed.

380 We selected the paired air and water passive samples collected in 2012  
381 autumn at Cape Vincent (On12-3503) as a case study, because in this case all  
382 three air-water exchange situations (i.e. deposition, volatilization and  
383 equilibrium) were observed. Contributions to variance in air-water exchange  
384 fluxes, air-water fugacity ratios and the fluxes of selected PCBs are list in Table 1.

385 Air-water fugacity ratios and probabilities of net deposition or volatilization  
386 indicate that primary trends of CB 28 and 52 were net deposition, those of CB  
387 138 and 153 were net volatilization, and those of CB 101, 118 and 180  
388 approached phase equilibrium. The parameter sensitivities were related with  
389 air-water exchange situation of PCBs, combining with Equation 4. When  
390 air-water exchange was approaching an equilibrium situation, uncertainty in  
391 air-water exchange flux was primarily controlled by the uncertainty in  $H_c$ ,  $C_a$  and  
392  $C_w$ . Their assumed normal probability distributions would result in symmetrical  
393 probability distribution of the flux in Figures S3.c and d. In non-equilibrium  
394 situations, uncertainty in wind speed propagated largely to uncertainty in the  
395 flux and led to a large tail of its probability distribution (see Figure S3.a, b, e and  
396 f). The flux uncertainty was related to uncertainty in  $C_w$  in net volatilization  
397 situation (e.g. CB 138 and 153), but related to uncertainties in  $C_a$  and  $H_c$  in net  
398 deposition situation (e.g. CB 28 and 52).

399 **Air-water exchange flux of total PCBs across the whole lakes.** After  
400 estimating site-specific air-water exchange fluxes of PCBs, we fitted PDFs of  
401 atmospheric and aqueous concentrations of PCBs and calculated probability  
402 distribution of air-water exchange flux across each entire lakes via Monte Carlo  
403 simulation (see Figure 4 and Table S3). Histograms of site-specific air-water  
404 exchange fluxes across Lakes Erie and Ontario are also illustrated in Figure 4. In  
405 both lakes, the calculated probability distributions via Monte Carlo simulation  
406 agreed well with the histograms. Across the whole Lake Erie, the calculated  
407 fluxes of total PCBs within a confidence level of 90% ranged from  $-5.1 \text{ ng m}^{-2}$   
408  $\text{day}^{-1}$  (net deposition) to  $52 \text{ ng m}^{-2} \text{ day}^{-1}$  (net volatilization), and MLE, median  
409 and mean values were  $0.78 \text{ ng m}^{-2} \text{ day}^{-1}$ ,  $3.4 \text{ ng m}^{-2} \text{ day}^{-1}$  and  $11.7 \text{ ng m}^{-2} \text{ day}^{-1}$ ,

410 respectively. The probability of net volatilization ( $F_{a/w} > 0$ ) was 84%.  
411 Contributions of aqueous and atmospheric concentrations, wind speed and  
412 temperature were 87%, 7%, 4% and 0.7% of the flux variability, respectively. A  
413 similar result was observed across the whole Lake Ontario. The flux of total PCBs  
414 (confidence level of 90%) ranged from  $-3.0 \text{ ng m}^{-2} \text{ day}^{-1}$  (net deposition) to  $68 \text{ ng}$   
415  $\text{m}^{-2} \text{ day}^{-1}$  (net volatilization), and MLE, median and mean values were  $0.53 \text{ ng m}^{-2}$   
416  $\text{day}^{-1}$ ,  $3.6 \text{ ng m}^{-2} \text{ day}^{-1}$  and  $13.6 \text{ ng m}^{-2} \text{ day}^{-1}$ , respectively. The probability of net  
417 volatilization was 87%. Contributors are same with those in Lake Erie,  
418 accounting for 84%, 11%, 4% and 0.6% of the flux variability, respectively.

419 **Gross volatilization loss of PCBs.** If the probability distribution of air-water  
420 exchange flux mentioned above were acceptable, gross volatilization loss could  
421 be calculated by the product of surface area and arithmetic mean of the flux.  
422 Annual volatilization losses of total PCBs in the whole lake were 74 kg for Lake  
423 Erie and 63 kg for Lake Ontario (detailed in Table S3). Although the MLE of  
424 air-water exchange fluxes were frequently approached, the gross loss was  
425 significantly elevated by a few extremely large values of the volatilization flux  
426 (see Figure S1). It is noteworthy that the simulated probability distribution, to  
427 some extent, covered temporal and spatial variation of air-water exchange flux of  
428 PCBs across the whole lakes, especially under extreme conditions, e.g., gale.

429 **Mass balance of PCBs.** For the purpose of understanding the relative  
430 importance of air-water exchange of total PCBs, a mass balance of  
431 freely-dissolved PCBs in Lake Ontario was constructed. Annual input and output  
432 masses are presented in Figure 5 and Table S4. Compared mass loss via the St.  
433 Lawrence River ( $4.46 \pm 4.37 \text{ kg year}^{-1}$ ), volatilization of PCBs from water to air  
434 ( $63 \text{ kg year}^{-1}$ ) was the major loss pathway. Surprisingly, the annual loss was not

435 balanced by the inputs from the Niagara River ( $12.4 \pm 6.9$  kg year<sup>-1</sup>), other rivers  
436 ( $\sim 0.6 \pm 0.3$  kg year<sup>-1</sup>) and precipitation ( $\sim 0.56 \pm 0.44$  kg year<sup>-1</sup>). The parameters  
437 sensitivity analysis discussed above indicated that uncertainty in aqueous  
438 concentration is the primary contributor (84%) to the variation of air-water  
439 exchange flux of PCBs across Lake Ontario. Our previous study suggested that  
440 river discharge and localized influences likely dominated spatial distribution of  
441 aqueous PCBs in both lakes.<sup>8</sup> Hence, the reason for more PCBs volatilizing from  
442 the lake surface than entering from rivers and deposition is probably attributed  
443 to uninvolved contributions from other large tributaries (e.g., rivers of Humber,  
444 Credit and Nappanee), land based sources (e.g., waste water treatment plant and  
445 urban runoff) and (resuspended) sediment releasing PCBs back to water phase.  
446 Nevertheless, further effort is warranted to evaluate their contributions.

447

## 448 **IMPLICATIONS**

449 The estimation of uncertainty in air-water exchange fluxes of PCBs is a challenge  
450 because many measurement with considerable uncertainty are involved. Besides  
451 the filter bias of active sampling, in theory, there is not significant difference in  
452 calculation of air-water flux at specific sites for active and passive sampling, if  
453 PCBs reached equilibrium between passive sampler and ambient air (or water).  
454 Air-water fluxes across the lower Great Lakes are constantly changing over time  
455 and space. Yet the high cost of active sampling significantly restricts our ability to  
456 assess the spatial variation of air-water exchange flux at a large scale, such as  
457 across Lakes Erie and Ontario. The deployment of passive sampler at a high  
458 geospatial resolution could overcome these restrictions. In theory, passive  
459 sampling technology can more precisely evaluate the direction of air-water

460 exchange of lighter PCBs because of lower relative uncertainty in %equilibrium.  
461 Although Monte Carlo simulations were successfully used to estimate  
462 uncertainty in air-water exchange of PCBs across the whole lakes, some  
463 limitations affected also this study. For example, few samplers were deployed in  
464 the open lake and along the Canadian shore. In addition, temperature  
465 dependence of atmospheric concentration of PCBs failed to be defined in the  
466 Monte Carlo simulation. Fugacity and net flux are related to ambient  
467 temperature. Increasing temperatures enhance the volatilization flux due to  
468 temperature corrections to the partitioning coefficient between air and water  
469 (major) and water-side mass transfer coefficient (minor). Spatial variations in  
470 wind speed over both lakes were ignored in this case, assuming that they were  
471 minor over open-lake areas, which makes up most of the total surface area of the  
472 Great Lakes.

473

#### 474 **ASSOCIATED CONTENT**

##### 475 **Supporting Information**

476 Detailed information on error propagation analysis and Monte Carlo simulation  
477 can be found along with calculated gross volatilization loss and mass balance of  
478 PCBs in the lakes. This material is available free of charge via the Internet at  
479 [Http://pubs.acs.org](http://pubs.acs.org).

480

#### 481 **AUTHOR INFORMATION**

##### 482 **Corresponding Author.**

483 \* E-mail: [lohmann@gso.uri.edu](mailto:lohmann@gso.uri.edu)

##### 484 **Notes**

485 The authors declare no competing financial interest.

486

## 487 **ACKNOWLEDGEMENTS**

488 We acknowledge funding from EPA's Great Lakes Restoration Initiative Award

489 GLAS No. 00E00597-0 (Project Officer Todd Nettesheim) supporting passive

490 sampler research in the Great Lakes, the Foundation of State Key Laboratory of

491 Pollution Control and Resource Reuse (No.: PCRRY15013) and the Shanghai

492 Science and Technology Commission (No. 16ZR1438100). We thank Dave

493 Adelman (URI) and our cast of volunteers for passive sampler deployments

494 around Lakes Erie and Ontario and the field staff of the Emergencies, Operational

495 Analytical Laboratories, and Research Support group (Environment Canada

496 Burlington) for open-lake deployments, and the Ontario Ministry of the

497 Environment for near-shore deployments along Lake Ontario.

498

## 499 **REFERENCES:**

500 1. Melymuk, L.; Robson, M.; Csiszar, S. A.; Helm, P. A.; Kaltenecker, G.; Backus, S.; Bradley, L.;  
501 Gilbert, B.; Blanchard, P.; Jantunen, L. From the city to the lake: Loadings of PCBs, PBDEs,  
502 PAHs and PCMs from Toronto to Lake Ontario. *Environ. Sci. Technol.* **2014**, *48* (7),  
503 3732-3741.

504 2. Salamova, A.; Venier, M.; Hites, R. A. Revised Temporal Trends of Persistent Organic  
505 Pollutant Concentrations in Air around the Great Lakes. *Environmental Science &*  
506 *Technology Letters* **2015**, *2* (2), 20-25.

507 3. Binational.net Canada and the United States Designate the First Set of Chemicals of  
508 Mutual Concern. <https://binational.net/2016/05/31/cmcdesig-pcpmdesig/>

509 4. Eisenreich, S. J.; Looney, B. B.; Thornton, J. D. Airborne organic contaminants in the Great  
510 Lakes ecosystem. *Environ. Sci. Technol.* **1981**, *15* (1), 30-38.

511 5. Jiménez, J. C.; Dachs, J.; Eisenreich, S. J. Chapter 8 – Atmospheric Deposition of POPs:  
512 Implications for the Chemical Pollution of Aquatic Environments. *Comprehensive*  
513 *Analytical Chemistry* **2015**, *67*, 295-322.

514 6. Bidleman, T. F.; McConnell, L. L. A Review of Field Experiments to Determine Air-Water  
515 Gas-Exchange of Persistent Organic Pollutants. *Sci. Total. Environ.* **1995**, *159* (2-3),  
516 101-117.

517 7. Hornbuckle, K. C.; Jeremiason, J. D.; Sweet, C. W.; Eisenreich, S. J. Seasonal-Variations in

- 518 Air-Water Exchange of Polychlorinated-Biphenyls in Lake-Superior. *Environ. Sci. Technol.*  
519 **1994**, *28* (8), 1491-1501.
- 520 8. Liu, Y.; Wang, S.; McDonough, C. A.; Khairy, M.; Muir, D. C.; Helm, P. A.; Lohmann, R.  
521 Gaseous and Freely-Dissolved PCBs in the Lower Great Lakes Based on Passive Sampling:  
522 Spatial Trends and Air-Water Exchange. *Environ. Sci. Technol.* **2016**, *50* (10), 4932-9.
- 523 9. Ruge, Z.; Muir, D.; Helm, P.; Lohmann, R. Concentrations, Trends, and Air-Water Exchange  
524 of PAHs and PBDEs Derived from Passive Samplers in Lake Superior in 2011. *Environ. Sci.*  
525 *Technol.* **2015**, *49* (23), 13777-13786.
- 526 10. Schwarzenbach, R. P.; Gschwend, P. M.; Imboden, D. M. *Environmental Organic Chemistry*  
527 *(2nd edition)*. Wiley Interscience: USA, 2002.
- 528 11. Tidwell, L. G.; Allan, S. E.; O'Connell, S. G.; Hobbie, K. A.; Smith, B. W.; Anderson, K. A.  
529 Polycyclic Aromatic Hydrocarbon (PAH) and Oxygenated PAH (OPAH) Air-Water  
530 Exchange during the Deepwater Horizon Oil Spill. *Environ. Sci. Technol.* **2015**, *49* (1),  
531 141-149.
- 532 12. Gigliotti, C. L.; Brunciak, P. A.; Dachs, J.; Glenn, T. R.; Nelson, E. D.; Totten, L. A.; Eisenreich,  
533 S. J. Air-water exchange of polycyclic aromatic hydrocarbons in the New York-New Jersey,  
534 Usa, Harbor Estuary. *Environ. Toxicol. Chem.* **2002**, *21* (2), 235-244.
- 535 13. Swackhamer, D. L.; Schottler, S.; Pearson, R. F. Air-water exchange and mass balance of  
536 toxaphene in the great lakes. *Environ. Sci. Technol.* **1999**, *33* (21), 3864-3872.
- 537 14. Nelson, E. D.; McConnell, L. L.; Baker, J. E. Diffusive exchange of gaseous polycyclic  
538 aromatic hydrocarbons and polychlorinated biphenyls across the air-water interlace of  
539 the Chesapeake Bay. *Environ. Sci. Technol.* **1998**, *32* (7), 912-919.
- 540 15. Qin, N.; He, W.; Kong, X. Z.; Liu, W. X.; He, Q. S.; Yang, B.; Ouyang, H. L.; Wang, Q. M.; Xu, F. L.  
541 Atmospheric partitioning and the air-water exchange of polycyclic aromatic  
542 hydrocarbons in a large shallow Chinese lake (Lake Chaohu). *Chemosphere* **2013**, *93* (9),  
543 1685-1693.
- 544 16. Blanchard, P.; Audette, C. V.; Hulting, M. L.; Basu, I.; Brice, K.; Backus, S.; Dryfhout-Clark, H.;  
545 Froude, F.; Hites, R.; Nielson, M.; Wu, R. *Atmospheric Deposition of Toxic Substances to the*  
546 *Great Lakes: IADN Results through 2005*. US EPA and Environment Canada, US EPA  
547 905-R-08-001.: 2008; p 226.
- 548 17. Rowe, M. D.; Perlinger, J. A. Micrometeorological measurement of hexachlorobenzene and  
549 polychlorinated biphenyl compound air-water gas exchange in Lake Superior and  
550 comparison to model predictions. *Atmos. Chem. Phys.* **2012**, *12* (10), 4607-4617.
- 551 18. Fang, M. D.; Ko, F. C.; Baker, J. E.; Lee, C. L. Seasonality of diffusive exchange of  
552 polychlorinated biphenyls and hexachlorobenzene across the air-sea interface of  
553 Kaohsiung Harbor, Taiwan. *Sci. Total. Environ.* **2008**, *407* (1), 548-565.
- 554 19. Cheng, J. O.; Ko, F. C.; Lee, C. L.; Fang, M. D. Air-water exchange fluxes of polycyclic  
555 aromatic hydrocarbons in the tropical coast, Taiwan. *Chemosphere* **2013**, *90* (10),  
556 2614-2622.
- 557 20. Lin, T.; Guo, Z.; Li, Y.; Nizzetto, L.; Ma, C.; Chen, Y. Air-Seawater Exchange of  
558 Organochlorine Pesticides along the Sediment Plume of a Large Contaminated River.  
559 *Environ. Sci. Technol.* **2015**, *49* (9), 5354-62.
- 560 21. Wang, X.; Nagpure, A. S.; DeCarolis, J. F.; Barlaz, M. A. Characterization of Uncertainty in  
561 Estimation of Methane Collection from Select U.S. Landfills. *Environ. Sci. Technol.* **2015**, *49*



- 562 (3), 1545-1551.
- 563 22.Venier, M.; Hites, R. A. Atmospheric deposition of PBDEs to the Great Lakes featuring a  
564 Monte Carlo analysis of errors. *Environ. Sci. Technol.* **2008**, *42* (24), 9058-64.
- 565 23.Khairy, M.; Muir, D.; Teixeira, C.; Lohmann, R. Spatial Distribution, Air-Water Fugacity  
566 Ratios and Source Apportionment of Polychlorinated Biphenyls in the Lower Great Lakes  
567 Basin. *Environ. Sci. Technol.* **2015**, *49* (23), 13787-97.
- 568 24.Lohmann, R.; Muir, D. Global Aquatic Passive Sampling (AQUA-GAPS): Using Passive  
569 Samplers to Monitor POPs in the Waters of the World. *Environmental Science &*  
570 *Technology* **2010**, *44* (3), 860-864.
- 571 25.Khairy, M.; Muir, D.; Teixeira, C.; Lohmann, R. Spatial Trends, Sources, and Air-Water  
572 Exchange of Organochlorine Pesticides in the Great Lakes Basin Using Low Density  
573 Polyethylene Passive Samplers. *Environ. Sci. Technol.* **2014**, *48* (16), 9315-9324.
- 574 26.Blanchard, P.; Audette, C. V.; Hulting, M. L.; Basu, I.; Brice, K. A.; Backus, S. M.;  
575 Dryfhout-Clark, H.; Froude, F.; Hites, R. A.; Neilson, M. *Atmospheric deposition of toxic*  
576 *substances to the Great Lakes: IADN results through 2005*. Environment Canada Burlington:  
577 2008; p 226.
- 578 27.Mackay, D. *Multimedia environmental models: the fugacity approach*. CRC press: 2001.
- 579 28.Wang, Y.; Luo, C. L.; Wang, S. R.; Liu, J. W.; Pan, S. H.; Li, J.; Ming, L. L.; Zhang, G.; Li, X. D.  
580 Assessment of the Air-Soil Partitioning of Polycyclic Aromatic Hydrocarbons in a Paddy  
581 Field Using a Modified Fugacity Sampler. *Environ. Sci. Technol.* **2015**, *49* (1), 284-291.
- 582 29.Luo, X. L.; Zheng, Y.; Lin, Z. R.; Wu, B.; Han, F.; Tian, Y.; Zhang, W.; Wang, X. J. Evaluating  
583 potential non-point source loading of PAHs from contaminated soils: A fugacity-based  
584 modeling approach. *Environ. Pollut.* **2015**, *196*, 1-11.
- 585 30.Castro-Jimenez, J.; Berrojalbiz, N.; Wollgast, J.; Dachs, J. Polycyclic aromatic hydrocarbons  
586 (PAHs) in the Mediterranean Sea: Atmospheric occurrence, deposition and decoupling  
587 with settling fluxes in the water column. *Environ. Pollut.* **2012**, *166*, 40-47.
- 588 31.Zhong, G. C.; Xie, Z. Y.; Moller, A.; Halsall, C.; Caba, A.; Sturm, R.; Tang, J. H.; Zhang, G.;  
589 Ebinghaus, R. Currently used pesticides, hexachlorobenzene and hexachlorocyclohexanes  
590 in the air and seawater of the German Bight (North Sea). *Environ. Chem.* **2012**, *9* (4),  
591 405-414.
- 592 32.Mulder, M. D.; Heil, A.; Kukucka, P.; Klanova, J.; Kuta, J.; Prokes, R.; Sprovieri, F.; Lammel, G.  
593 Air-sea exchange and gas-particle partitioning of polycyclic aromatic hydrocarbons in the  
594 Mediterranean. *Atmos. Chem. Phys.* **2014**, *14* (17), 8905-8915.
- 595 33.Jantunen, L. M.; Wong, F.; Gawor, A.; Kylin, H.; Helm, P. A.; Stern, G. A.; Strachan, W. M. J.;  
596 Burniston, D. A.; Bidleman, T. F. 20 Years of Air-Water Gas Exchange Observations for  
597 Pesticides in the Western Arctic Ocean. *Environ. Sci. Technol.* **2015**, *49* (23),  
598 13844-13852.
- 599 34.Bruhn, R.; Lakaschus, S.; McLachlan, M. S. Air/sea gas exchange of PCBs in the southern  
600 Baltic Sea. *Atmos. Environ.* **2003**, *37* (24), 3445-3454.
- 601 35.Lammel, G.; Audy, O.; Basis, A.; Efstathiou, C.; Eleftheriadis, K.; Kohoutek, J.; Kukucka, P.;  
602 Mulder, M. D.; Pribylova, P.; Prokes, R.; Rusina, T. P.; Samara, C.; Sofuoglu, A.; Sofuoglu, S.  
603 C.; Tasdemir, Y.; Vassilatou, V.; Voutsas, D.; Vrana, B. Air and seawater pollution and air-sea  
604 gas exchange of persistent toxic substances in the Aegean Sea: spatial trends of PAHs,  
605 PCBs, OCPs and PBDEs. *Environ. Sci. Pollut. R.* **2015**, *22* (15), 11301-11313.

- 606 36.Lohmann, R.; Gioia, R.; Jones, K. C.; Nizzetto, L.; Temme, C.; Xie, Z.; Schulz-Bull, D.; Hand, I.;  
607 Morgan, E.; Jantunen, L. Organochlorine Pesticides and PAHs in the Surface Water and  
608 Atmosphere of the North Atlantic and Arctic Ocean. *Environ. Sci. Technol.* **2009**, *43* (15),  
609 5633-5639.
- 610 37.Zhong, G.; Xie, Z.; Cai, M.; Moller, A.; Sturm, R.; Tang, J.; Zhang, G.; He, J.; Ebinghaus, R.  
611 Distribution and air-sea exchange of current-use pesticides (CUPs) from East Asia to the  
612 high Arctic Ocean. *Environ. Sci. Technol.* **2012**, *46* (1), 259-67.
- 613 38.Fang, M. D.; Lee, C. L.; Jiang, J. J.; Ko, F. C.; Baker, J. E. Diffusive exchange of PAHs across the  
614 air-water interface of the Kaohsiung Harbor lagoon, Taiwan. *J. Environ. Manage.* **2012**,  
615 *110*, 179-87.
- 616

617

618 Table 1. Contributions to variation of air-water exchange flux, fugacity ratios,  
 619 mass fluxes ( $\text{ng m}^{-2} \text{ day}^{-1}$ ), certainties in deposition or volatilization of  
 620 selected 7 PCBs at Cape Vincent (On12) in 2012 autumn.

621

Variables	PCB28	PCB52	PCB101	PCB118	PCB138	PCB153	PCB180
<b>(Parameter sensitivity analysis)</b>							
PCB in air	<b>-0.28</b>	<b>-0.26</b>	<b>-0.25</b>	<b>-0.39</b>	-0.07	-0.09	<b>-0.20</b>
$H_c$	<b>0.60</b> <sup>a</sup>	<b>0.55</b>	<b>0.58</b>	<b>0.52</b>	0.15	0.22	<b>0.35</b>
PCB in water	0.08	0.10	<b>0.52</b>	<b>0.50</b>	<b>0.55</b>	<b>0.55</b>	<b>0.59</b>
Temperature	-0.12	-0.13	-0.01	-0.01	0.10	0.09	0.06
Wind Speed	<b>-0.55</b>	<b>-0.61</b>	0.03	0.09	<b>0.64</b>	<b>0.60</b>	<b>0.45</b>
<b>(Estimation of air-water exchange situation)</b>							
$\log(f_a/f_w)$ <sup>b</sup>	0.34	0.44	-0.04	-0.09	-0.83	-0.98	-0.53
Flux <sup>c</sup>	-0.54	-0.23	0.01	0.02	0.1	0.09	0.02
Certainty <sup>d</sup>	95%	97%	51%	56%	92%	94%	83%
Situation	Deposition		Equilibrium		Volatilization		Equilibr.

622 <sup>a</sup>, Major contributors to the variance are marked by Bold.

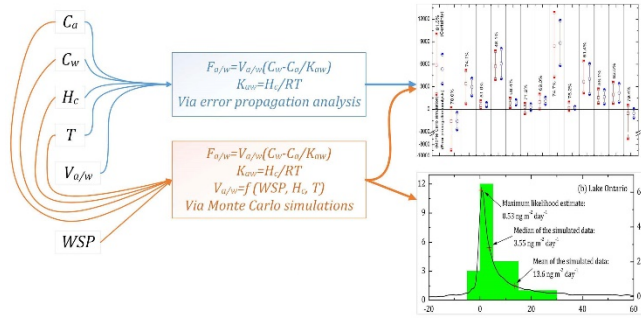
623 <sup>b</sup>, Table S2 in the Supporting Information indicated the range of ratios where air water  
 624 exchange does not significant deviate from equilibrium.

625 <sup>c</sup>, Negative presents for deposition and positive for volatilization, unit:  $\text{ng m}^{-2} \text{ day}^{-1}$ ;

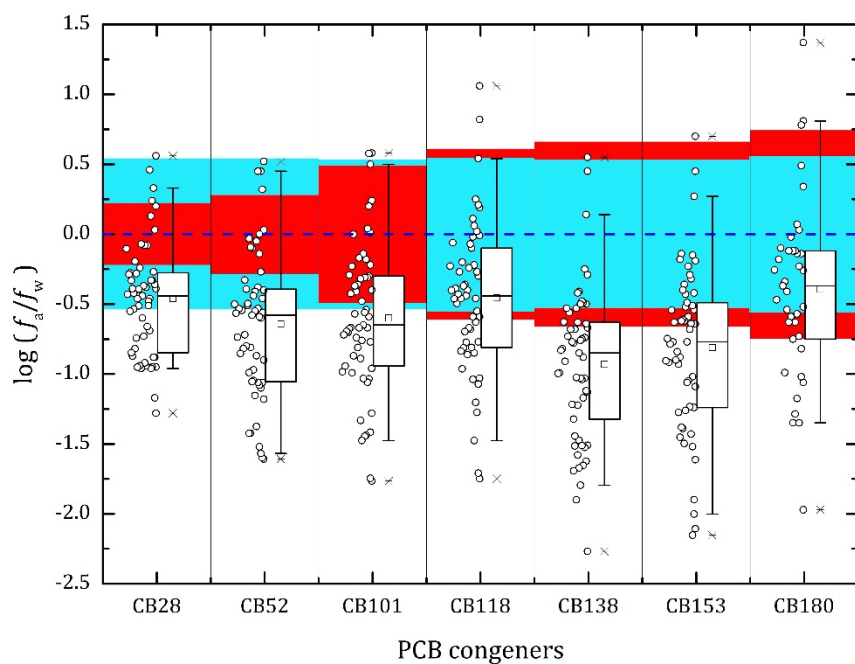
626 <sup>d</sup>, Certainty of net deposition or net volatilization, probability distributions of the fluxes are  
 627 illustrated in Figure S3;

628

629 TOC  
 630 (Size: 8.47cm x 4.24 cm)



631



632

633 Figure 1. Log-transformed air-water fugacity ratios of selected 7 PCBs. Blue dash line

634 presents equilibrium between air and water theoretically. Red and cyan regions

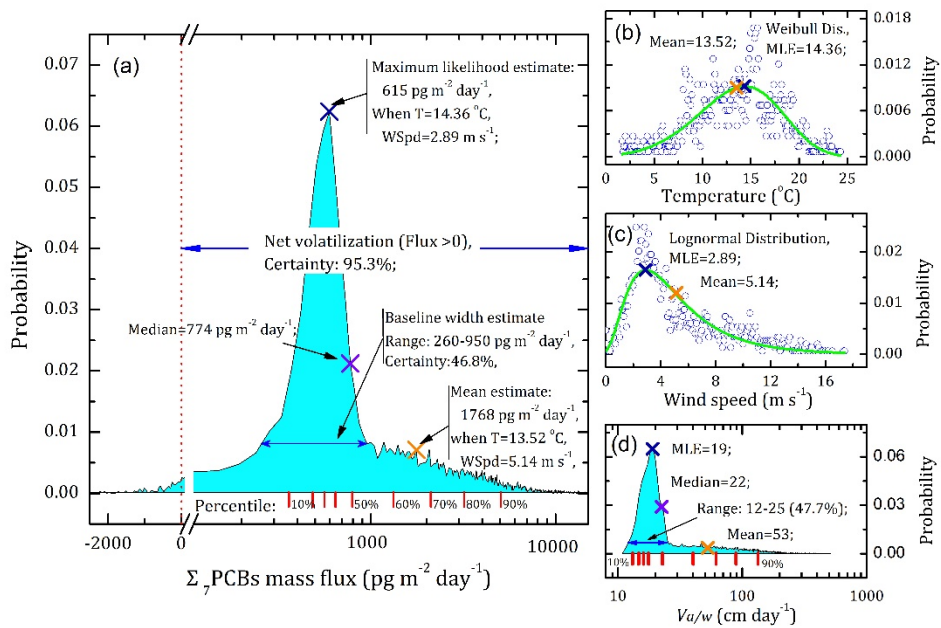
635 indicate the range that air-water exchange does not significant deviate from

636 equilibrium, based on Equations 7 and 8, respectively.

637

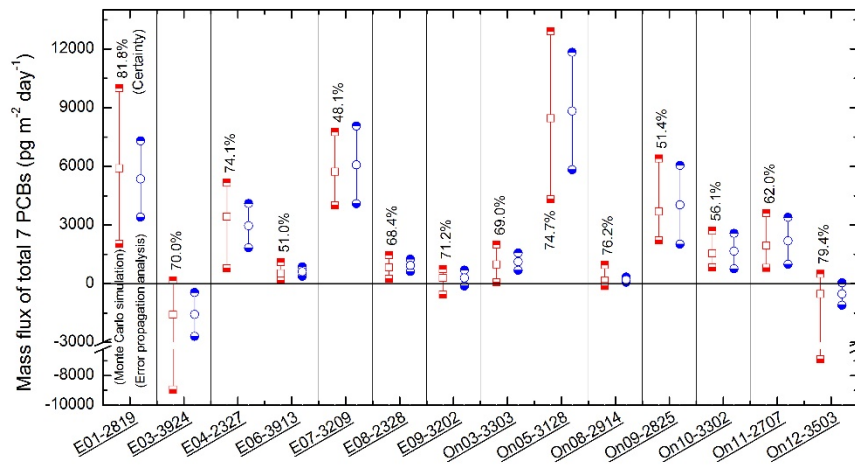
638

639  
640



641  
642  
643  
644  
645  
646  
647  
648

Figure 2. Total air-water exchange flux of 7 selected PCBs from Monte Carlo simulation. Black, orange and violet crosses present maximum likelihood estimation (MLE), arithmetic mean and median values, respectively. Temperature followed a Weibull distribution, and wind speed was fitted well by a lognormal distribution.



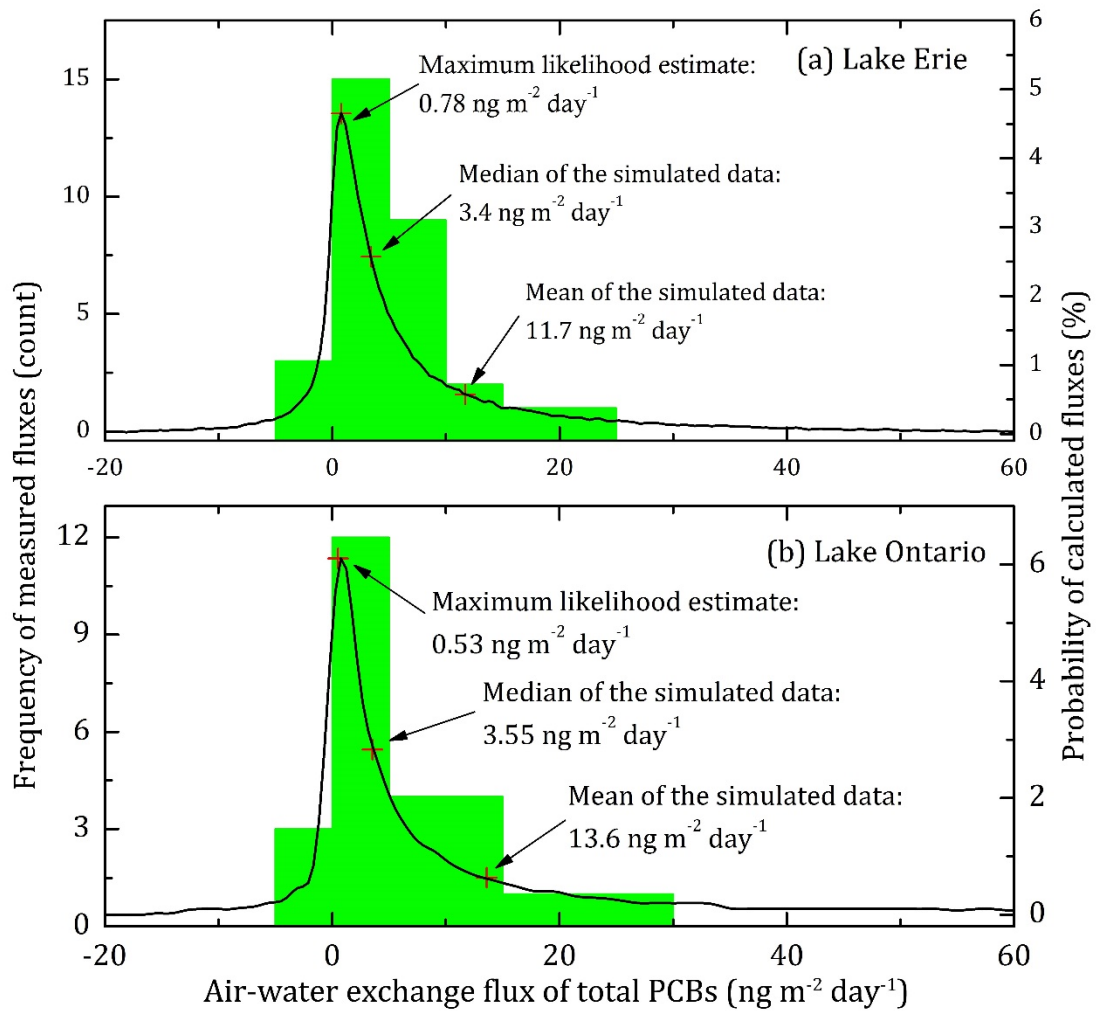
650

651 Figure 3. Best estimates (open) and uncertainty ranges (half solid) of air-water exchange  
 652 flux of  $\Sigma_7$ PCBs for fourteen selected samples. Certainties in good estimation range of  
 653 the flux and uncertainty ranges between red squares were determined based on  
 654 Monte Carlo simulation. The uncertainty ranges between blue circles were quantified  
 655 by error propagation analysis.

656

657

658

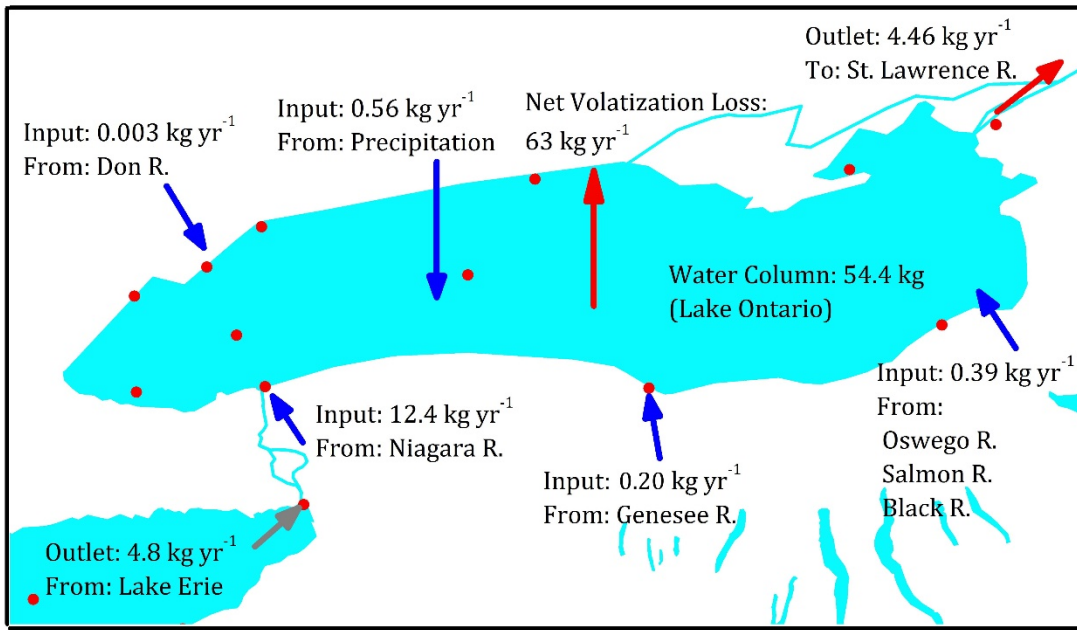


659  
 660  
 661  
 662  
 663

Figure 4. Monte Carlo-simulated probability distribution and measured frequency histogram of air-water exchange flux of total PCBs across Lake Erie (a) and Ontario (b).



664



665

666 Figure 5. Mass balance of PCBs in Lake Ontario. Blue and red arrows present annual input  
667 and output of freely-dissolved PCBs.

668

669